Actuators

DOI: 10.1002/anie.201303757

Dynamic Single Crystals: Kinematic Analysis of Photoinduced Crystal Jumping (The Photosalient Effect)**

Panče Naumov, Subash Chandra Sahoo, Boris A. Zakharov, and Elena V. Boldyreva**

During the process of evolution, animals and plants have naturally acquired two capabilities that are of critical importance for their survival: to evolve and to disperse. Natural motility is a mechanistically complex and very diverse phenomenon. Animal locomotion on solid surfaces, for instance, includes walking, running, jumping (hopping), and crawling (slithering).[1] Living plants, such as conifers, develop strains in their tissue by generating cell stress, which drives organ motility.[2] Other plants, such as the Venus flytrap or mimosa, rapidly actuate their organs for nutrition or defense by active mechanisms that are directed by architectural change of cellulose fibrils in a hygroscopic swelling matrix.[3,4] Seeds of certain plant species, which are effectively dead, disperse by a variety of mechanisms powered by periodic changes of humidity, such as crawling, creeping, ratcheting, and passive or active ballistic actions that are triggered by explosive fractures, swelling, twisting, buckling, and snapping.[5] Such passive motility provides models for prototypic mechanisms for bioinspired self-actuating devices.[6]

Unlike the mechanistically extremely complex tissues of animals, plants, and plant seeds, actuation and motility are far less intuitive and rather unanticipated for simple physical objects of homogeneous composition. Two insurmountable difficulties for the actual application of photoactuated elastomeric materials to mimic biogenic actuators, rooted in the inherently low degree of coupling between the thermal/light energy and mechanical energy, are their slow operation and extended recovery time from the actuated state. Actuating nematic liquid-crystalline polymers are generally characterized by less-than-optimal directionality vectors and low-order parameters; with polymer-based photomechanical actuators these characteristics translate into inefficient and slow energy conversion.

We hypothesized that these impediments could be surmounted by utilizing molecular single crystals, which can mimic the motions of active (tissues, organs) and passive (seeds) dynamic elements of plants and animals at the macroscopic level. At the same time, the systems allow one to mimic the photomechanical effects in biological processes at the microscopic level. Many proteins are light-sensitive, light absorption triggers conformational changes and large mechanical motions, and this plays an important role in their function.[7–10] The dense and ordered structure of crystalline molecular solids provides a platform for cooperative action and faster energy transfer with low energy dissipation and enhanced coupling between light and mechanical energy. Notably, certain organic and metal–organic molecular crystals have favorable elastic moduli, and although they normally experience stronger force for the same displacement and undergo small absolute deformations, extraordinary local photoresponsive stresses can be anticipated. Such crystalline actuators could be employed in practice for energy harvesting, tunable contact printing, mechanical actuation in artificial muscles, as microfluidic valves and gates or mechanically tunable optical elements, and in switchable reflector elements for projective displays, among other things.[11]

We report herein that when excited with strong cw UV light, micrometer- to millimeter-sized prismatic crystals of $[Co(NH_3)_5(NO_2)]Cl(NO_3)$ (**1**-*N*) suddenly hop off the surface and travel up to several tens of centimeters, that is, 10^2–10^5 times their own length (Figure 1). By analogy to the respective thermally induced jumping,[12–23] we suggest the term "photosalient effect" for this photomechanical phenomenon. The effect is not intuitively expected for a simple inorganic compound with a discrete ionic structure such as **1**-*N*, and it represents the visually most impressive macroscopic manifestation of the stress that can develop in response to the mechanical force created inside a crystal as a result of miniscule structure perturbation, by sudden release of the collective energy through the concerted action of the intermolecular interactions at the molecular level.[24]

Irradiation by light of nitropentaamminecobalt(III) complexes with various anions is known to result in intramolecular linkage isomerization that affords nitrito isomers such as $[Co(NH_3)_5(ONO)]Cl(NO_3)$ (**1**-*O*) where the ligand is coordinated through the oxygen atom. The reaction has been extensively studied[25–35] (reference [36] provides the most comprehensive overview on the topic). In contrast to many other solid-state transformations that involve nucleation and propagation of the reaction interface,[37,38] this reaction proceeds homogeneously through formation of solid solutions $(\mathbf{1}\text{-}N)_{1-x}(\mathbf{1}\text{-}O)_x$ $(x<1)$ without any phase separation, as was confirmed by visual microscopic observations,[30] as well as by in situ monitoring of the reaction with X-ray analysis.[34,35] Because of light absorption by the crystal, the distribution of

[*] Prof. P. Naumov, Dr. S. C. Sahoo
New York University Abu Dhabi
PO Box 129188, Abu Dhabi (United Arab Emirates)
E-mail: pance.naumov@nyu.edu
Dr. B. A. Zakharov, Prof. E. V. Boldyreva
Institute of Solid State Chemistry and Mechanochemistry
Siberian Branch of Russian Academy of Sciences
ul. Kutateladze, 18, Novosibirsk 630128 (Russia)
and
Novosibirsk State University
ul. Pirogova, 2, Novosibirsk 630090 (Russia)
E-mail: eboldyreva@yahoo.com

[**] P.N. thanks NYUAD for financial support.
Supporting information for this article is available on the WWW under http://dx.doi.org/10.1002/anie.201303757.

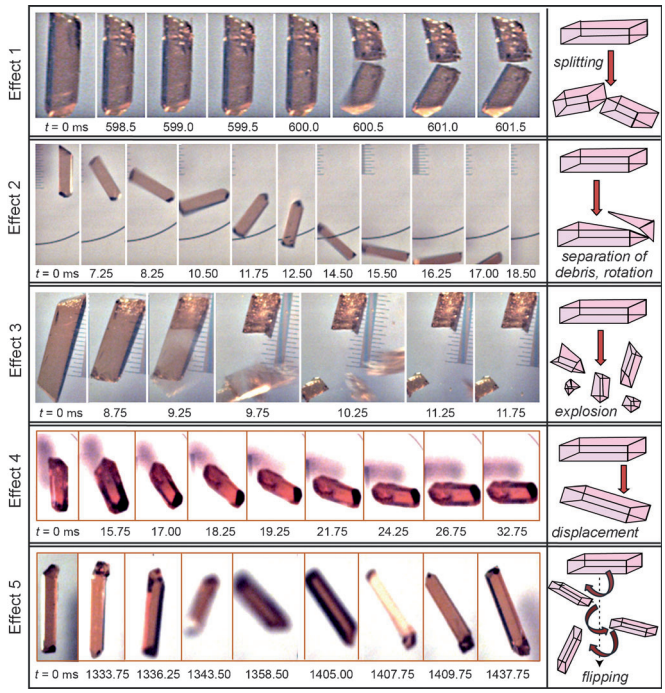

Figure 1. Series of snapshots and sketches of the five kinematic effects of UV-excited crystals of **1**-*N*: Splitting of a crystal into two pieces of nearly equal size (1), separation of a small piece off the crystal that propels the remaining part into a spinning or linear motion (2), crystal explosion (3), minor repositioning without lift off the base and apparent splitting or separation of debris (4), and rolling or flipping of the crystal (5). Typical high-speed recordings of these effects were deposited as Supporting Information (Movies S3–S11).

reaction product is nonuniform along the direction normal to the irradiated face, but is otherwise homogeneous in each layer. Concurrently, stress is accumulated to a certain critical value, followed by relaxation that appears as fragmentation, cooperative rotation of molecular fragments, molecules, or extension/switching of precompressed hydrogen bonds.

1-*N* can be crystallized from aqueous solutions as thin needles (for example, in the presence of a habit-forming additive (polyvinyl alcohol)). When exposed to light with $\lambda =$ 254–560 nm normal to the longest axis (which in standard orthorhombic *Pnma* setting with $b \approx 7.3$ Å coincides with the *b* axis of the unit cell), these crystals are known to visibly bend,[30] with the convex site directed towards the incident light. The deformation of the crystals is directly proportional to the number of the absorbed light quanta and depends on the exposure to the incident excitation, H_e ($H_e = P_d \times t_{exp}$, where P_d is the power density and t_{exp} is the exposure time; Figure S1 in the Supporting Information). The bending is elastic and completely reversible, and the bent crystals remain clear and transparent. The original shape of the crystals can be recovered by thermal treatment owing to the reverse thermal nitrito-to-nitro isomerization. The recovery time is inversely related to the temperature; the crystals recover their original shape in 6 h at 20 °C, but the recovery time can be shortened down to 2.5 h at 50 °C and even to 1 min at 100 °C.[39]

We observed that recrystallization of **1**-*N* from aqueous solutions in the absence of additive affords crystals of a second habit: well-shaped, orange crystalline blocks. The prismatic crystals have an identical structure with the needle-like crystals, however, upon irradiation with moderately strong UV light ($\lambda_{max} = 365$ nm) they did not bend. Instead, they displayed a dramatic mechanical effect: the crystals hopped suddenly and vigorously in a nonconcerted manner and in seemingly random directions, occasionally landing several centimeters from their original position (Movie S1 in the Supporting Information). Some crystals underwent minor but instantaneous dislocation before hopping, while others propelled themselves multiple times before taking off the base.

For kinematic analysis of the photoinduced self-actuation in **1**-*N*, a total of more than 250 crystals were individually excited with UV light in several regimes and individually examined with a high-speed camera coupled to a reflectivity-mode optical microscope. Each crystal was laid flat with its largest face on a smooth micrometer glass plate at a fixed angle relative to the top-incident UV light. At incident power density $P_d = 63\ mW\,cm^{-2}$, all crystals were mechanically responsive to excitation. A series of 2D snapshots were recorded with a time-resolution of 250 μs with the camera perpendicular to the microscopic stage and individually analyzed. Representative snapshots are shown in Figure 1.

Analysis of the image sequences recorded from the first batch of 40 individual crystals that were excited at constant power density P_d and spatial disposition to the incident light unraveled that the hopping is preceded by a latent stage where strain accrues and the crystals remain still (see panels A and B in Figure 2). At $P_d = 63\ mW\,cm^{-2}$, the latent period of strain tolerance (t_{lat}) varied between 0.59950 s and 4.44825 s, and did not depend individually on the width, length and thickness of the crystals. Instead, the strain tolerance was determined by the crystal volume (V) and the cross-section (σ) normal to the longest crystal axis (Figure 2A,B). At short accrual times t_{lat}, only small crystals hopped. The probability of larger crystals being actuated increased with longer exposures. For a hypothetical set of crystals of identical volume, there was a shortest time ($t_{lat,min}$) required to accumulate sufficient stress for actuation, and an upper time limit ($t_{lat,max}$) by which all crystals must jump. The shortest period of stress tolerance ($t_{lat,min}$) increased with the crystal volume (cross-section). Whereas small crystals were susceptible to a large range of stresses and could move after short excitation as well as during prolonged exposure, large crystals remained immobile at short excitation and required longer exposure to accumulate sufficient stress for a mechanical response. Consequently, small crystals would be desirable for faster photomechanical actuation, although a wider distribution of mechanical response times is to be anticipated.

The separators $t_{lat,min}$ in the V–t_{lat} and σ–t_{lat} plots in Figure 2A and 2B set the boundary to the region where crystal motion is feasible (at $63\ mW\,cm^{-2}$, $t_{lat,min}\,s^{-1} = 2.3 \times 10^{-8}\ V_{ave}\,\mu m^{-3}$). In the unpopulated region, the mechanical actuation is physically impossible and the motion is forbidden. These limiting conditions are determined by the susceptibility of the material to internal strain and represent direct

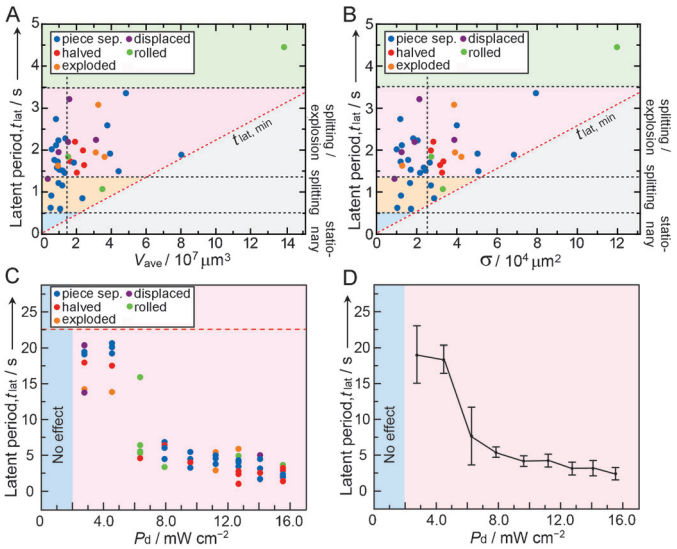

Figure 2. Stress-tolerance plots (A, B) and effect of the excitation power density (P_d) (C, D) on the photosalient effect in **1**-*N* crystals. The latent period (t_{lat}) for stress accrual where the crystal remains still depends on the crystal volume (V_{ave}; A) and the cross section (σ; B). The plots in panels A and B also show that the photosalient effect is physically unfeasible in the forbidden region below the separator designated $t_{lat,min}$. Plots C and D (the latter includes the standard deviation) indicate that a threshold value in the excitation power density is required to trigger the photosalient effect.

Table 1: Classes of basic photosalient kinematic effects and traceable patterns in crystals of **1**-*N*.

Basic motion effects (see Figure 1)	Label	Movie No.
Splitting in pieces of nearly equal size	1	S3
Separation of small piece(s)	2	S4, S5
Crystal explosion	3	S6, S7
Displacement without apparent splitting or lift off	4	S8, S9
Rolling or flipping	5	S10, S11
Traceable motion patterns (see Figures 3 and 4)	**Label**	
Displacement by slow rotation	*1*	
Displacement by fast rotation	*2*	
Rotation around one terminus owing to debris separation, followed by propelling and/or rotation	*3*	
Propelling quasiparallel to the longest crystal axis	*4*	
Complex motion	*5*	
Shifting	*6*	
Very fast rotation of pieces due to explosion	*7*	

experimental evidence of the physical limits to the time required for mechanical response in photosalient solids.

Two critical factors responsible for the impressive leaping of the **1**-*N* crystals are the sizeable accumulated strain and the time scale on which the debris separates. Indeed, actuation can occur only if a sizeable amount of anisotropically accumulated strain is released within a very short time interval. The high-speed recordings showed that any cracking and separation of debris from the **1**-*N* crystals occurs in less than 0.1 µs (Movie S2, SI). By individual inspection of each crystal motion pattern, we have identified five basic kinematic effects of photomechanical response, effects 1–5 in Table 1 and in Figure 1. High-speed recordings of the five effects are typified in the movies S3–S11 in the Supporting Information. The locomotion of some complex crystals included a dramatic sequence of several consecutive effects, and this was particularly evident with crystal multiplets (Movies S12 and S13 in the Supporting Information).

Since some of the crystals underwent complex motions including two or three different effects consecutively, for better description of the kinematic patterns the crystal trajectories were tracked by approximating each crystal with a vector that connects three equidistant quasi-collinear points set along the bisector of the longest crystal axis (see Movies S14–S17 in the Supporting Information). Based on the trace appearance, we classified the five motion effects into seven kinematic patterns *1*–*7* (Table 1) by which any simple or complex motion of a **1**-*N* crystal can be described. The seven kinematic traces of motion patterns are typified by selected crystals in Figure 3, and all observed kinematic patterns are deposited as Figure S2 in the Supporting Information. The trajectories of the central point are depicted in Figure 4, and Figure S3 in the Supporting Information shows an overlapped representation of these trajectories. It is apparent from Figure 4 that with patterns *1*, *2*, and *4*, where the crystals do not undergo reorientation prior to the major leap (that is, they remain nearly parallel to the *y* axis in the plots) the motion occurs preferentially in the direction of the longest crystal axis and never normal to it. This preferred direction of motion is related to the anisotropy in the developed strain, which accumulates predominantly along the longest crystal axis. Expectedly, the trace spread is more pronounced in pattern *3*, where the crystal rotates before jumping, and especially with trajectories following the pattern *5* (complex composite motions).

Figure 2C shows the dependence on the excitation power density P_d of the average latent time studied on 51 crystals. For each excitation density, the latent period t_{lat} was averaged over several specimens to account for the size-dependence of the accrual time. For values of the power $P_d < 1$ mW cm^{-2}, the accumulated strain was insufficient to induce actuation, and the crystals did not jump even after 56 seconds of exposure. At $P_d = 3$ mW cm^{-2} the actuation did occur, but only after long exposure, between 13 and 22 seconds. Apparently, the photosalient effect can only occur above a certain threshold in the internal strain, which is determined by the time of exposure. By increasing the power density of the incident light the accrual time shortens, and for a higher incident power it depends linearly on the excitation density (Figure 2C). The correlation in this quasilinear section, $t_{lat} = -0.106\,P_d$, is only significant within $1.07\,\sigma$ owing to the spread introduced by the crystal size. Yet, Figure 2C shows another, much less intuitive correlation: the excitation power also determines the type of the photomechanical effect. At intermediate values of the excitation power range used here, rolling or flipping of the crystals (effect 5) was dominant. By increasing the power, separation of debris from the crystal (effect 2) became more frequent. At very high incident densities, most of the crystals were observed to split into pieces of comparable size (effect 1).

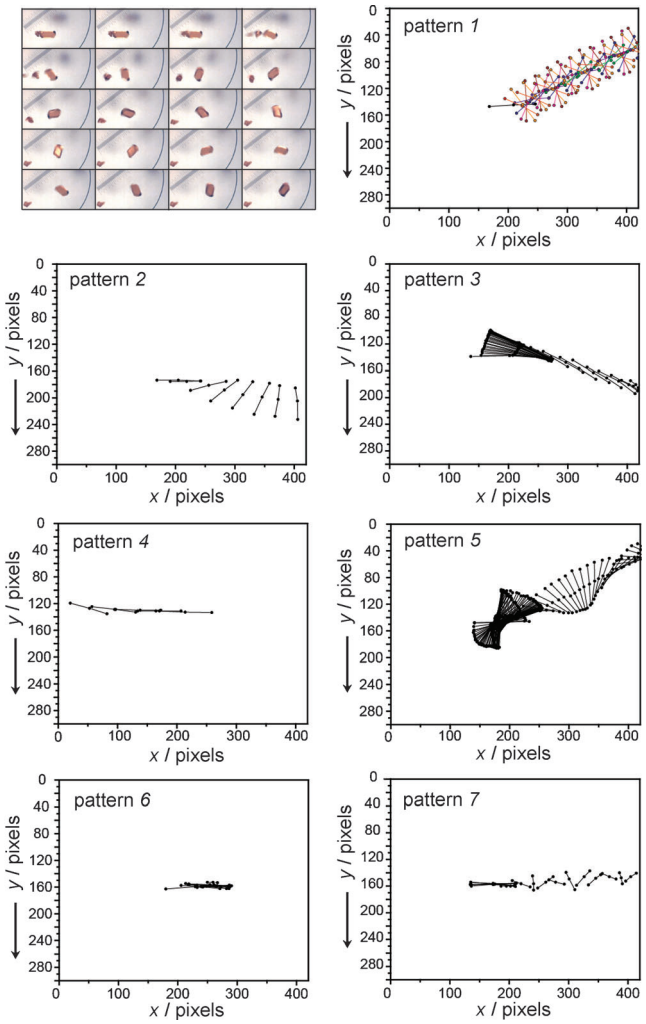

Figure 3. Typical traces of the seven kinematic patterns observed with the photosalient crystals of **1**-*N*. For tracking analysis, the crystals were approximated with a set of three quasicollinear points lying on the bisector of the longest crystal axis (see Movies S14–S17 in the Supporting Information). All coordinates are normalized to the initial position of the crystal barycenter, which was set at (200,150). The illustration on the top left typifies the motion of a crystal according to pattern *1* in 250 μs-time-resolved snapshots. The crystal orientations in the plot for pattern *1* are colored for clarity.

Two independent sets of experiments, measurement of the yield of **1**-*O* (IR spectroscopy) and of the bending angle of slender single crystals of **1**-*N* as a function of the energy exposition H_e (see above), have consistently shown that crystals of **1**-*N* break when about 20% of the molecules in the 20 μm thick surface layer are transformed to **1**-*O*, corresponding to a conversion of approximately 1–2% when calculated on the crystal bulk.[31] This result indicates that, provided the transformation of the crystal is spatially nonuniform, a miniscule overall yield is sufficient to trigger the effect.

To obtain an estimate of the order of magnitude of the basic kinematic parameters, we monitored the XY projection of the five basic types of motion of single crystals (14 specimens) during 1 s over small distances (3.5–130.7 mm) in the microscope field. The crystals moved with a value for the in-plane component of the speed on the order of $v_{xy} = 0.1$–$1\ \mathrm{m\,s^{-1}}$ and had the planar component of the kinetic energy $E_{k,xy} = 0.03$–44 nJ. Note that for small particles, such as the crystals of **1**-*N* studied here (0.3–$14 \times 10^{-11}\ \mathrm{m^3}$), the drag forces are substantial and are expected to reduce the theoretical height significantly.

The earlier attempts to quantify the excitation-dependent strain acquired by the lattice by isomerization to **1**-*O* of **1**-*N* were based on measurements of the curvature of bent crystals and the load required for mechanical disintegrations of the crystals during bending. The Young's modulus of approximately $10^{10}\ \mathrm{N\,m^{-2}}$ requires loads of approximately $10^{8}\ \mathrm{N\,m^{-2}}$ (0.1 GPa).[31] The internal strain was modeled by approximating the coordination cations of **1**-*N* transforming into **1**-*O* with isotropically expanding dilation centers, while accounting for a relative volume change $\Delta V/V \approx +20\%$ obtained from measurements in solution and nonhomogeneous distribution in the crystal bulk owing to depth-dependent light absorp-

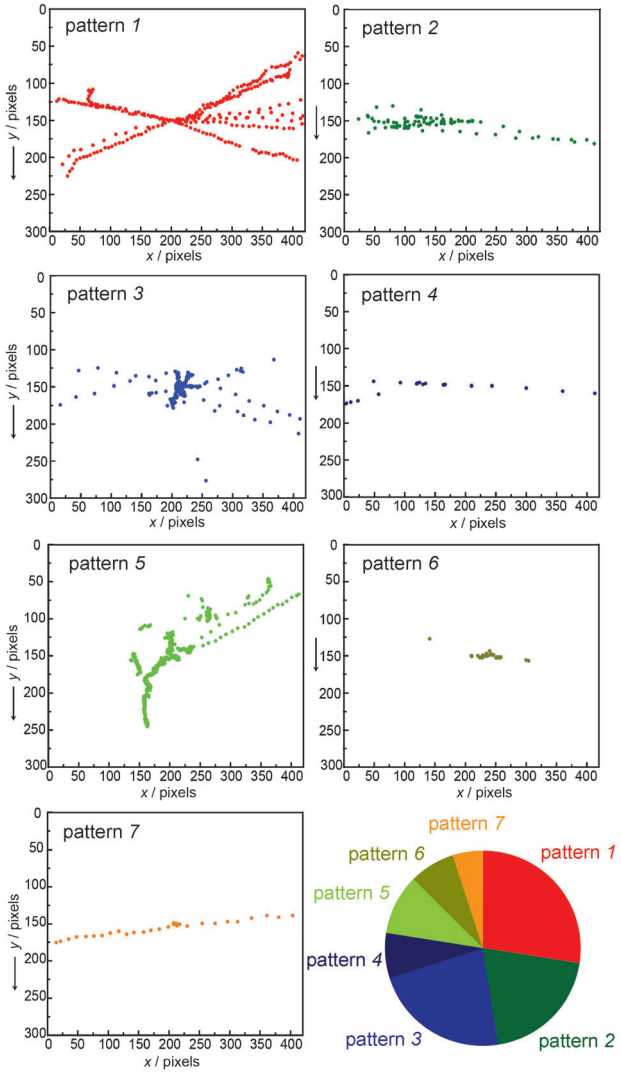

Figure 4. Seven types of trajectories of the central tracking point simulating the barycenters of **1**-*N* crystals that perform photosalient motions, and a pie-type plot showing the frequency of occurrence of the effects. The motion patterns are described in Table 1.

tion.[32] Despite being consistent with the observed direction of bending of the crystal, however, such a simple model was in discordance with the small negative change in molar volume observed by X-ray diffraction analysis for the transformation of **1**-*N* to **1**-*O* (−0.7%). This discrepancy was eventually explained by accounting for strain anisotropy, that is, by considering that the irradiated crystal expands +3.5% on irradiation along the crystallographic *b* axis, that coincides with the longest axis of elongated crystals in the *Pnma* setting, and contracts −2.34% and −1.8% in the directions normal to the longest axis of the crystal, along the crystallographic axes *a* and *c*, respectively.

Yet a model that assumes an exponential decrease of the concentration of the set of dilation centers perpendicular to the irradiated face, which also considers a homogenous distribution of these centers within a certain layer at the same distance from the surface, cannot substantiate the explosive-like fragmentation, the vast mechanical response, and complex macroscopic motions with a rotational momentum of thick crystals. Instead, these phenomena might result from cooperative action in the light-induced intramolecular rotation of the nitro groups within the arrays of regularly arranged coordination cations $[Co(NH_3)_5(NO_2)]^{2+}$ (Figure 5A). The threshold-like behavior of the effect observed with increasing excitation power (Figure 2C,D) is in support of a cooperative nature of the mechanism of the photosalient effect in **1**-*N*, however additional experimental evidence is required to substantiate this hypothesis.

Within a hypothetical cooperative-action model for the photosalient effect, we propose the following sequence of events. The rotation of the nitro group in the coordination cation following photoexcitation is related to the geometrical preferences of its different electronic states. The small intramolecular perturbation within the individual molecular fragments during linkage isomerization[36,40–43] is amplified along the three-dimensional hydrogen-bond network connecting the ions in the crystal that act as "springs" that accumulate the strain (Figure 5B).

We analyzed the rigidity of the molecular springs in an X-ray diffraction study of an **1**-*N* crystal exposed to external hydrostatic compression (for experimental details, see Tables S1 and S2 in the Supporting Information). On application of external pressures up to approximately 5 GPa, the distances between the non-hydrogen atoms within the N–H···O hydrogen bonds shortened 2–5% (0.06–0.12 Å) and those within the N–H···Cl hydrogen bonds shortened 3.5–7% (0.1–0.25 Å; see Figure 5C,D, and Table S2 in the Supporting Information). The two N–H···O hydrogen bonds bridging the two oxygen atoms (O1 and O2) of the nitro ligand with NH_3 ligands from adjacent cations differ in their geometry, and they also respond with different compressibility at high pressures. Being very long and weak, one of the two hydrogen bonds facilitates the rotation of the nitro group during the isomerization. The stress and strain imposed on the environment by the rotation of the nitro group are transferred from one cation to another through an infinite network of flexible hydrogen bonds that connect the NH_3 ligands with Cl^- and NO_3^- anions (Figure 5). These hydrogen bonds are capable of compression under external

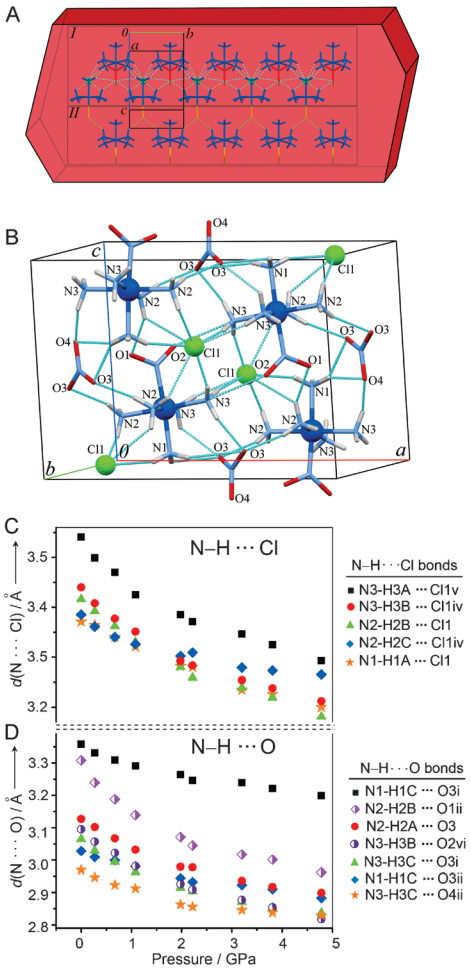

Figure 5. A) Relation between the crystal habit and packing in a crystal of $[Co(NH_3)_5(NO_2)]Cl(NO_3)$ (**1**-*N*). The direction of the long crystal axis is parallel with the crystallographic *b* axis. B) Fragment of the crystal structure of **1**-*N* with atom labeling and hydrogen bonds. C, D) Pressure-dependence of the distances between the non-hydrogen atoms participating in intermolecular hydrogen bonds. Symmetry code(s): (i) $x-1/2, y, -z+3/2$; (ii) $-x+1/2, -y, z-1/2$; (iii) $-x+1/2, y+1/2, z-1/2$; (iv) $-x+1/2, -y, z+1/2$; (v) $x-1/2, -y+1/2, -z+3/2$; (vi) $-x, y-1/2, -z+2$. See also Tables S1 and S2 in the Supporting Information.

hydrostatic pressure, as well as of expansion by the action of the internal pressure generated by photoisomerization. Since the nitro-to-nitrito photoisomerization results in a maximum linear strain of +3.5 Å, the internal pressure generated by the isomerization is estimated to several GPa. Notably, the increased external hydrostatic pressure is mostly reflected as compression along the crystallographic axis *b*, which expands in the course of the photoisomerization to **1**-*O*.

The vast mechanical macroscopic response that we observe with **1**-*N* is triggered by a miniscule change in the coordination site of a very small group (nitro ligand). This material provides one of the most extreme manifestations of self-actuation of single crystals. The capability to control the latent time by the excitation power and the size of the crystal provides a valuable probe into the limits of the mechanistic relationship between the atomic-scale structural perturba-

tions and their macroscopic consequences. In more general terms, the photosalient effect in the ballistic crystals of **1**-*N* represents a direct and visually impressive demonstration of the conversion of light into mechanical motion through a photochemical reaction on a macroscopic scale, which sets the platform for the design of fast biomimetic and technomimetic actuating materials that can mimic animal motions, dynamics of macromolecules, or dynamic technical elements.

Received: May 2, 2013
Revised: June 17, 2013
Published online: July 19, 2013

Keywords: actuators · biomimetic materials · isomers · jumping crystals · mechanical effects

[1] R. M. Alexander, *Principles of Animal Locomotion*, Princeton University Press, Oxford, **2006**.
[2] J. D. Boyd, *Aust. J. Biol. Sci.* **1950**, *3*, 270 – 293.
[3] Y. Forterre, J. M. Skotheim, J. Dumais, L. Mahadevan, *Nature* **2005**, *433*, 421 – 425.
[4] P. Fratzl, R. Elbaum, I. Burgert, *Faraday Discuss.* **2008**, *139*, 275 – 282.
[5] L. van der Pijl, *Dispersal in Higher Plants*, Springer, New York, **1982**, pp. 84 – 89.
[6] I. Burgert, P. Fratzl, *Philos. Trans. R. Soc. London Ser. A* **2009**, *367*, 1541 – 1557.
[7] H. Ihee, S. Rajagopal, V. Šrajer, R. Pahl, S. Anderson, M. Schmidt, F. Schotte, P. A. Anfinrud, M. Wulff, K. Moffat, *Proc. Natl. Acad. Sci. USA* **2005**, *102*, 7145 – 7150.
[8] M. Schmidt, T. Graber, R. Henning, V. Srajer, *Acta Crystallogr. Sect. A* **2010**, *66*, 198 – 206.
[9] S. Tripathi, V. Šrajer, N. Purwar, R. Henning, M. Schmidt, *Biophys. J.* **2012**, *102*, 325 – 332.
[10] A. B. Wohri, G. Kantona, I. C. Johansson, E. Fritz, E. Malmerber, M. Andersson, J. Vincent, M. Eklund, M. Cammarata, M. Wulff, et al., *Science* **2010**, *328*, 630 – 633.
[11] M. Behl, A. Lendlein, *Soft Matter* **2007**, *3*, 58 – 67.
[12] M. C. Etter, A. R. Siedle, *J. Am. Chem. Soc.* **1983**, *105*, 641 – 643.
[13] J. Gigg, R. Gigg, S. Payne, R. Conant, *J. Chem. Soc. Perkin Trans. 1* **1987**, 2411 – 2414.
[14] B. Kohne, K. Praefcke, G. Mann, *Chimia* **1988**, *42*, 139 – 141.
[15] T. Steiner, W. Hinrichs, R. Gigg, W. Saenger, *Z. Kristallogr.* **1988**, *182*, 252 – 253.
[16] J. Ding, R. Herbst, K. Praefcke, B. Kohne, W. Saenger, *Acta Crystallogr. Sect. B* **1991**, *47*, 739 – 742.
[17] J. Fattah, J. M. Twyman, C. M. Dobson, *Magn. Reson. Chem.* **1992**, *30*, 606 – 615.
[18] T. Steiner, W. Hinrichs, W. Saenger, R. Gigg, *Acta Crystallogr. Sect. B* **1993**, *49*, 708 – 718.
[19] S. Zamir, J. Bernstein, D. Greenwood, *Mol. Cryst. Liq. Cryst.* **1994**, *242*, 193 – 200.
[20] O. Crottaz, F. Kubel, H. Schmid, *J. Mater. Chem.* **1997**, *7*, 143 – 146.
[21] H. F. Lieberman, R. J. Davey, D. M. Newsham, *Chem. Mater.* **2000**, *12*, 490 – 494.
[22] Ž. Skoko, S. Zamir, P. Naumov, J. Bernstein, *J. Am. Chem. Soc.* **2010**, *132*, 14191 – 14202.
[23] R. Centore, M. Jazbinsek, A. Tuzi, A. Roviello, A. Capobianco, A. Peluso, *CrystEngComm* **2012**, *14*, 2645 – 2653.
[24] *Reactivity of Molecular Solids, Molecular Solid State Series, Vol. 3* (Eds.: E. V. Boldyreva, V. V. Boldyrev), Wiley, New York, **1999**, p. 342.
[25] B. Adell, *Z. Anorg. Allg. Chem.* **1955**, *279*, 219 – 224.
[26] W. W. Wendlandt, J. H. Woodlock, *J. Inorg. Nucl. Chem.* **1965**, *27*, 259 – 260.
[27] D. A. Johnson, K. A. Pashman, *Inorg. Nucl. Chem. Lett.* **1975**, *11*, 23 – 28.
[28] I. Grenthe, E. Nordin, *Inorg. Chem.* **1979**, *18*, 1869 – 1874.
[29] E. J. Rose, D. S. McClure, *J. Photochem.* **1981**, *17*, 171 – 171.
[30] E. V. Boldyreva, A. A. Sidel'nikov, A. P. Chupakhin, N. Z. Lyakhov, V. V. Boldyrev, *Proceed. Acad. Sci. USSR* **1984**, *277*, 893 – 896.
[31] E. V. Boldyreva, A. A. Sidel'nikov, *Proceed. Sib. Dept. Acad. Sci. USSR* **1987**, *5*, 139 – 145.
[32] B. I. Yakobson, E. V. Boldyreva, A. A. Sidel'nikov, *Proceed. Sib. Dept. Acad. Sci. USSR* **1989**, *51*, 6 – 10.
[33] E. V. Boldyreva, *Mol. Cryst. Liq. Cryst. Inc. Non-Lin. Opt.* **1994**, *242*, 17 – 52.
[34] E. V. Boldyreva, N. V. Podberezskaya, A. V. Virovets, L. P. Burleva, V. E. Dulepov, *J. Struct. Chem.* **1993**, *34*, 128 – 138.
[35] N. Masciocchi, A. N. Kolyshev, V. E. Dulepov, E. V. Boldyreva, A. Sironi, *Inorg. Chem.* **1994**, *33*, 2579 – 2585.
[36] E. V. Boldyreva, *Russ. J. Coord. Chem.* **2001**, *27*, 323 – 350.
[37] F. H. Herbstein, *Acta Crystallogr. Sect. B* **2006**, *62*, 341 – 383.
[38] T. P. Shakhtshneider, V. V. Boldyrev, *Solid State Ionics C* **1990**, *43*, 179 – 182.
[39] E. V. Boldyreva, A. A. Sidelnikov, N. I. Rukosuev, A. P. Chupakhin, N. Z. Lyakhov, Patent SU #1368654, **1985**.
[40] P. Coppens, I. Novozhilova, A. Kovalevsky, *Chem. Rev.* **2002**, *102*, 861 – 883.
[41] A. Y. Kovalevsky, G. King, K. A. Bagley, P. Coppens, *Chem. Eur. J.* **2005**, *11*, 7254 – 7264.
[42] M. R. Warren, S. K. Brayshaw, A. L. Johnson, S. Schiffers, P. R. Raithby, T. L. Easun, M. W. George, J. E. Warren, S. J. Teat, *Angew. Chem.* **2009**, *121*, 5821 – 5824; *Angew. Chem. Int. Ed.* **2009**, *48*, 5711 – 5714.
[43] L. E. Hatcher, M. R. Warren, D. R. Allan, S. K. Brayshaw, A. L. Johnson, S. Fuertes, S. Schiffers, A. J. Stevenson, S. J. Teat, C. H. Woodall, P. R. Raithby, *Angew. Chem.* **2011**, *123*, 8521 – 8524; *Angew. Chem. Int. Ed.* **2011**, *50*, 8371 – 8374.

